Supporting Informations

Metallic Layered Germanium Phosphide GeP_5 for High Rate Flexible All-Solid-State Supercapacitors

Bingchao Yang,[a] Anmin Nie,*[a] Yukai Chang,[a] Yong Cheng,[b] Fusheng Wen,*[a] Jianyong Xiang,[a] Lei Li,[c] Zhongyuan Liu,*[a] and Yongjun Tian[a]

[a]*State Key Laboratory of Metastable Materials Science and Technology, Yanshan University, Qinghuangdao 066004, China*
[b]*Department of Materials Science and Engineering, College of Materials, Xiamen University, Xiamen 361005, China*
[c]*Northwest Institute for Non-ferrous Metal Research, Xian 710016, China*

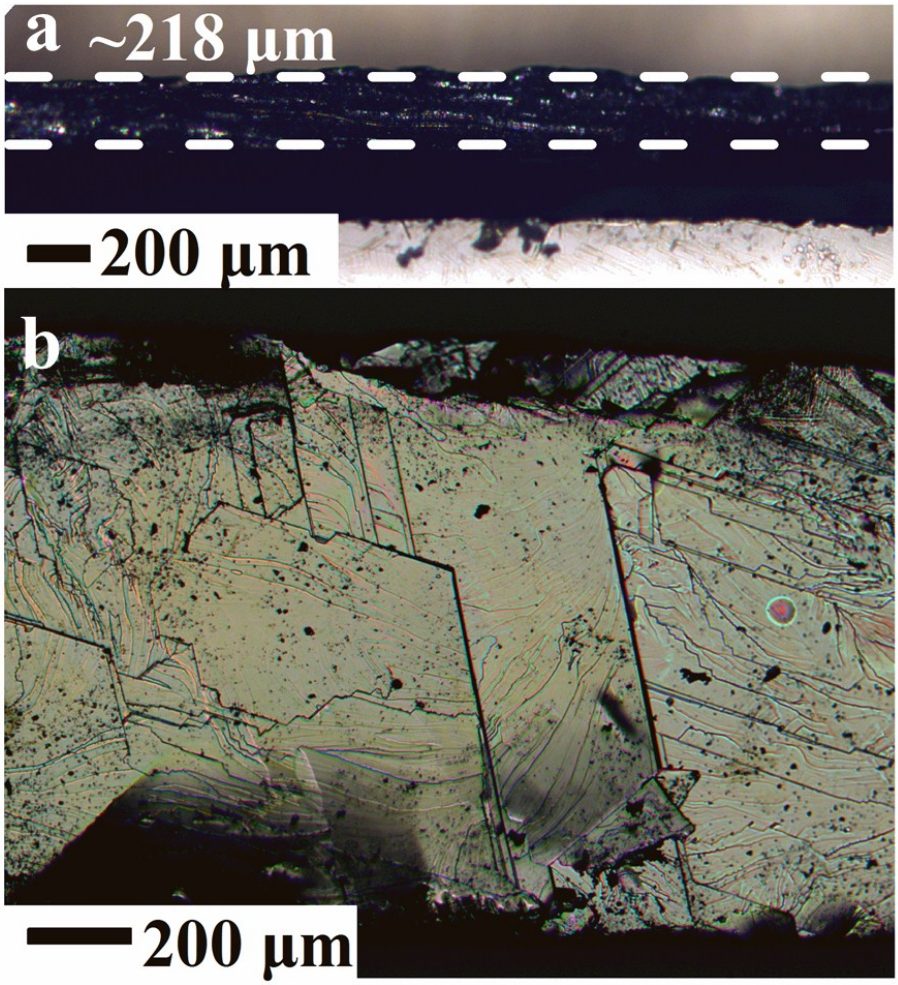

Figure S1 Optical Photographs of GeP_5 crystal piece used for temperature dependent electrical conductivity measurement. (a) Side view of the GeP_5 crystal piece. The thickness of the piece is about 1.1 mm. (b) The top view of the GeP_5 crystal piece.

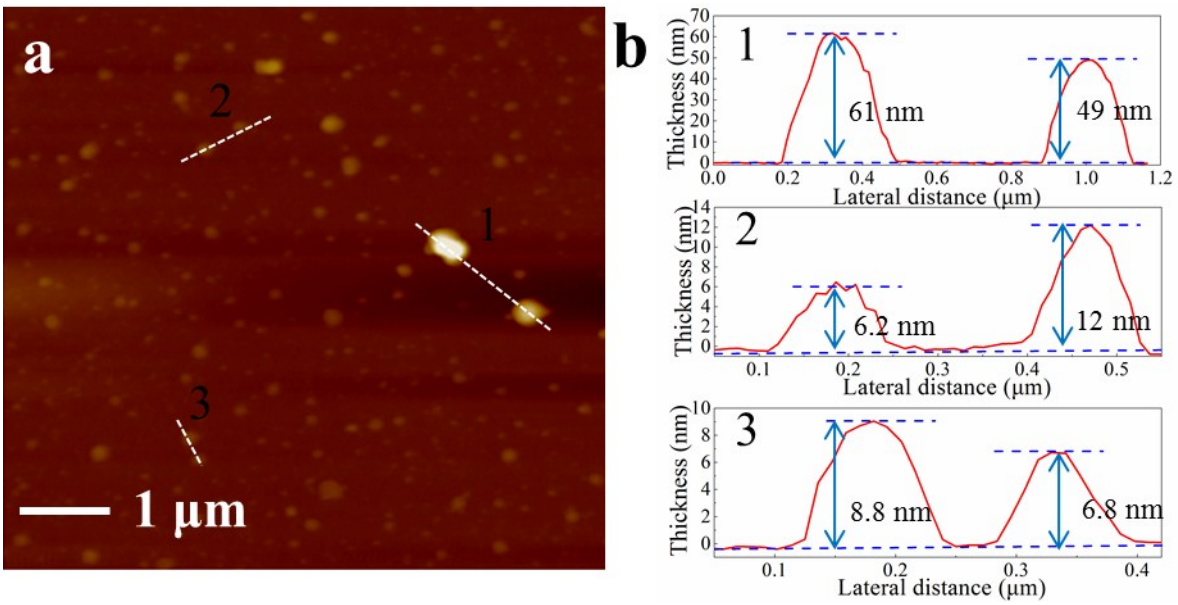

Figure S2 AFM characterization of the GeP_5 nanoflakes. (a) Representative AFM images of the GeP_5 nanoflakes. (b) The corresponding height profiles of the GeP_5 nanoflakes.

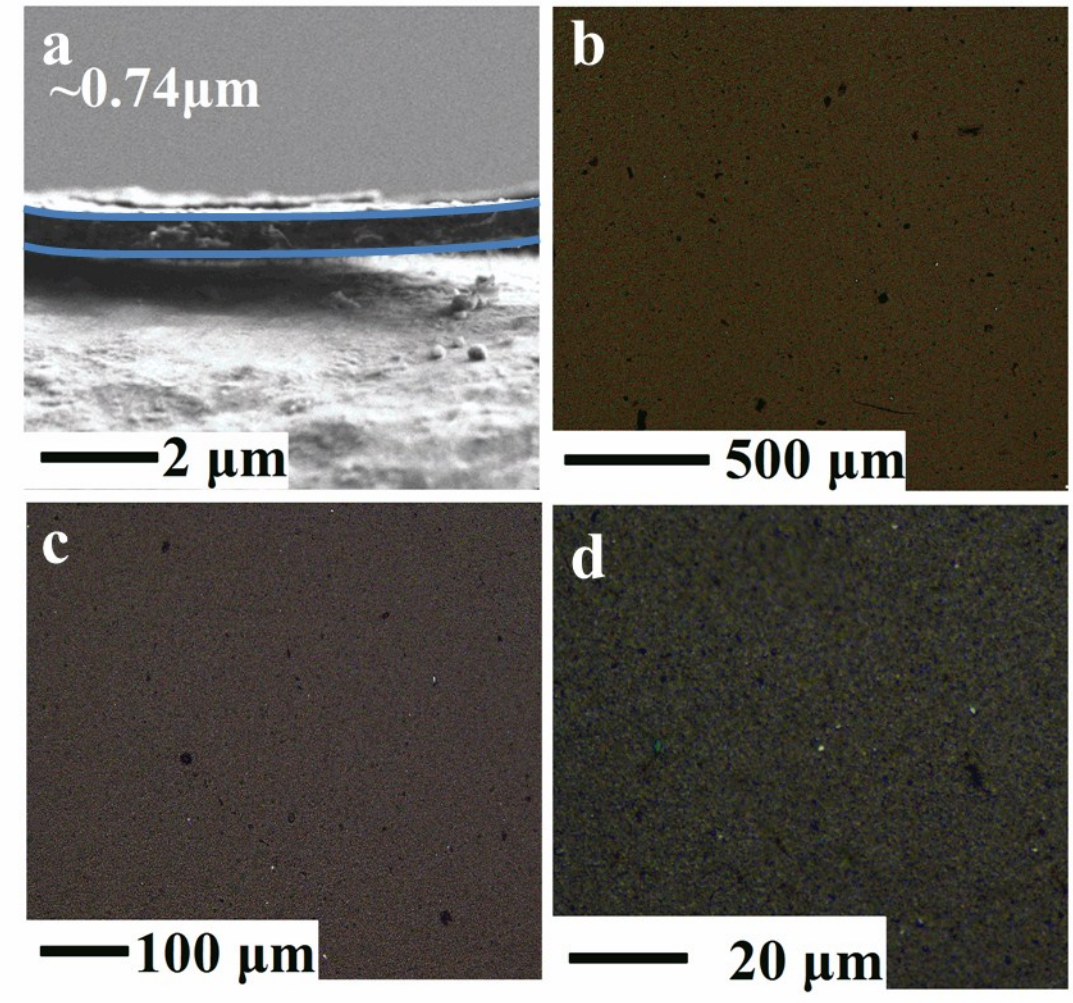

Figure S3 (a) Cross-section SEM image for GeP_5 film with a ~0.74 μm thickness composed by liquid-exfoliated GeP_5 nanoflakes. (b-d) Different magnification optical photographs showing the surface morphology of the GeP_5 film.

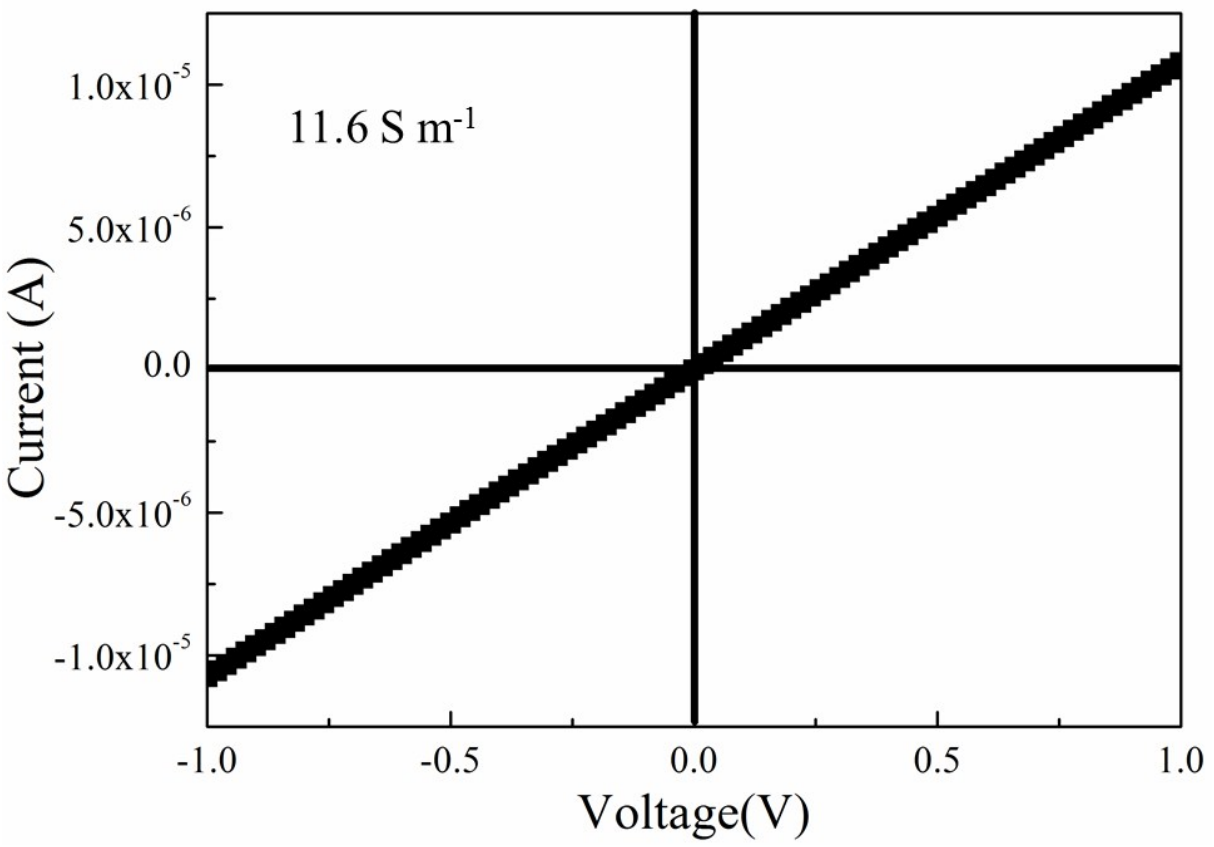

Figure S4 Resistivity test of GeP_5 film at room temperature in the voltage window from −1 to +1 V.

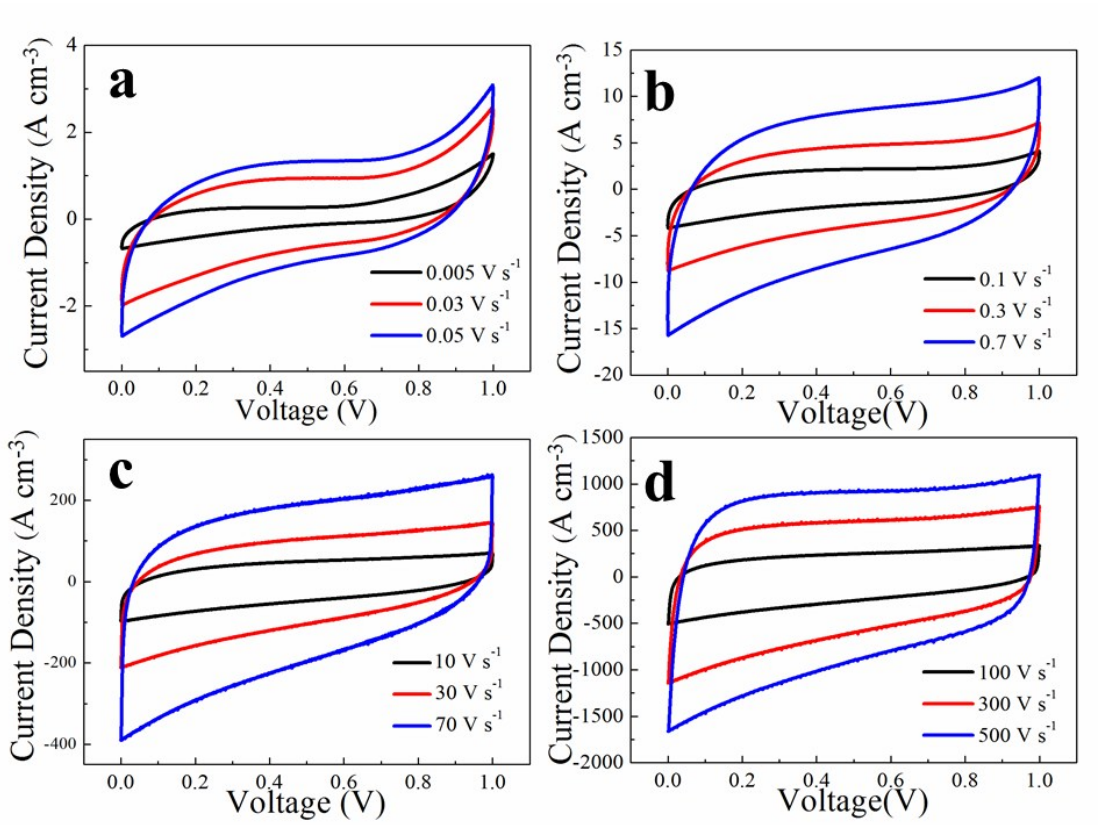

Figure S5 CV curves of the GeP_5 ASSP device at various scan rates range from 0.005 to 0.05 (a), 0.1 to 0.7 (b), 10 to 70 (c), and 100 to 500 V s^{-1} (d), respectively.

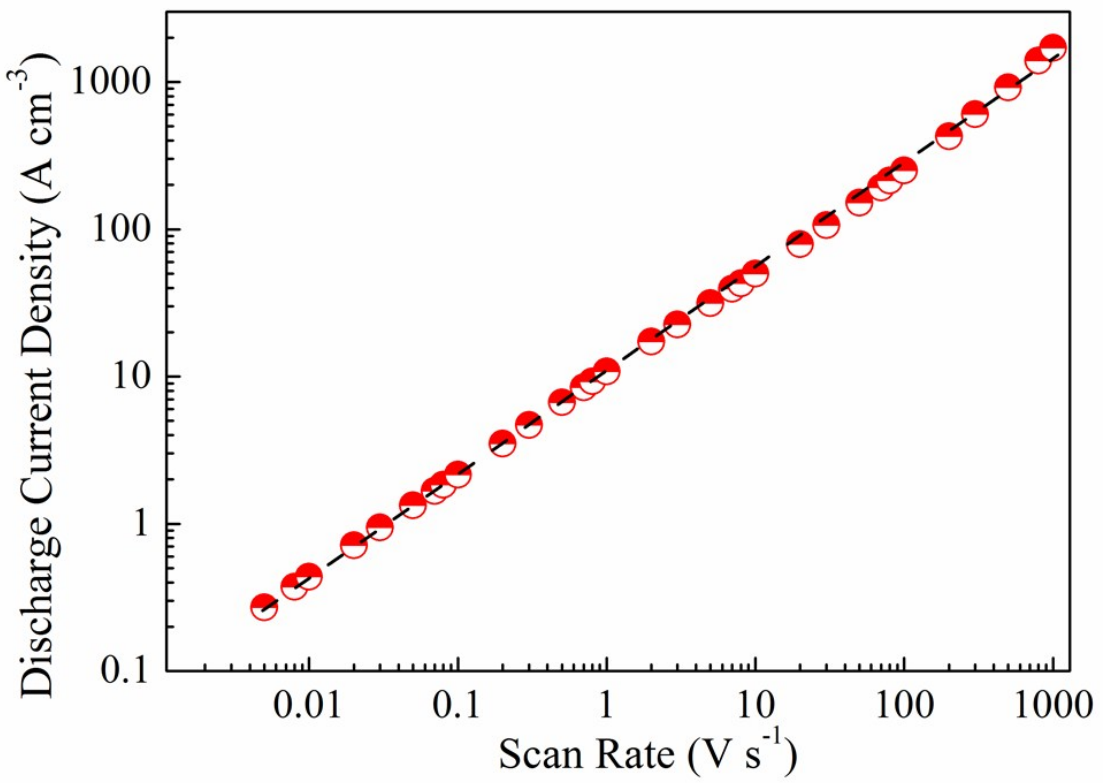

Figure S6 Plot of the discharge current density as a function of the scan rate for GeP_5 ASSP.

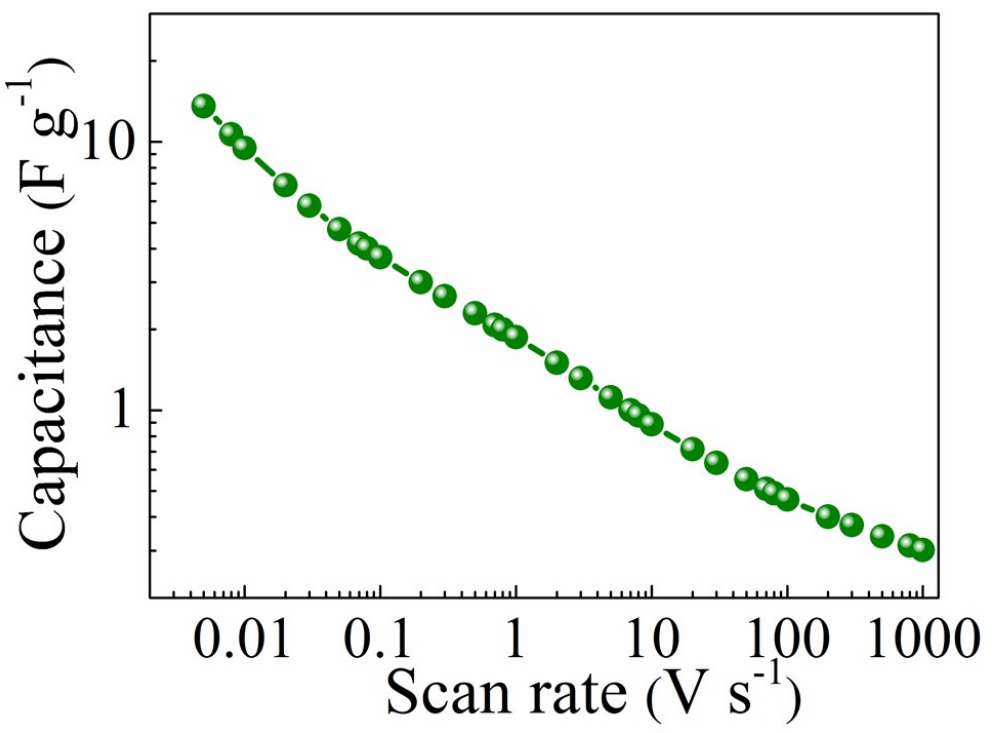

Figure S7 The gravimetric capacitance of GeP_5 ASSPs at different scan rates.

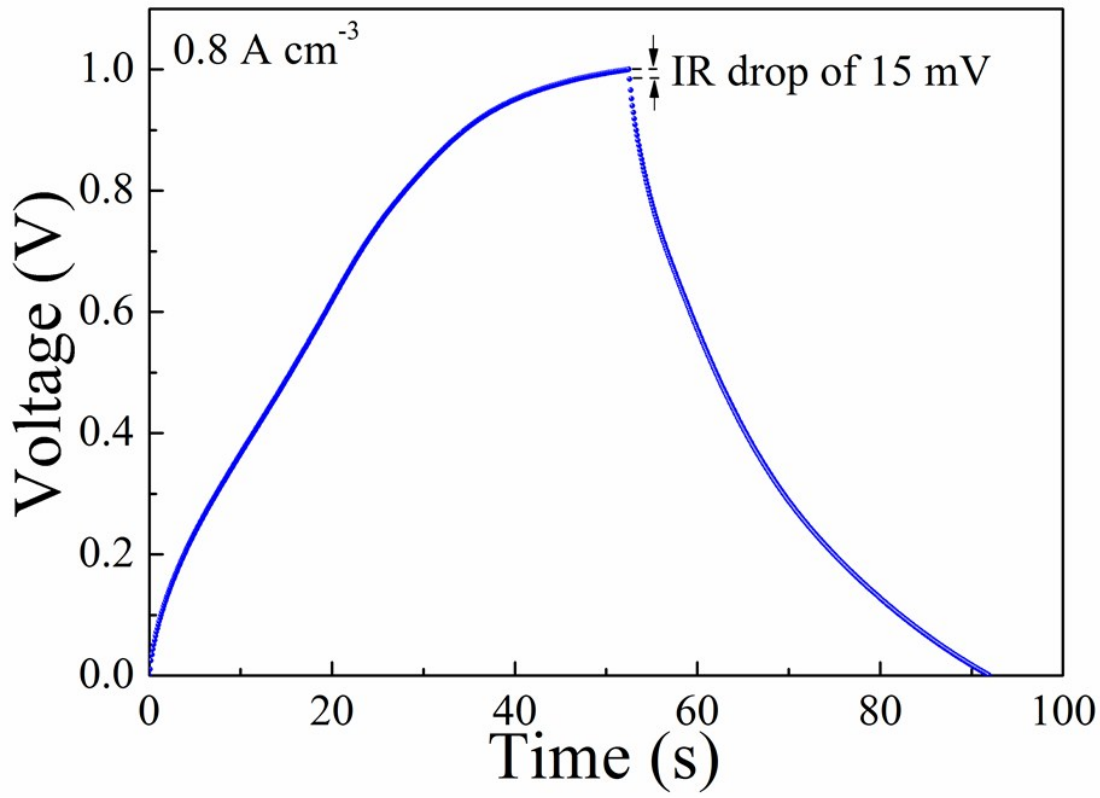

Figure S8 GCD curves at current density of 0.8 A cm^{-3} with a IR drop of 15 mV.

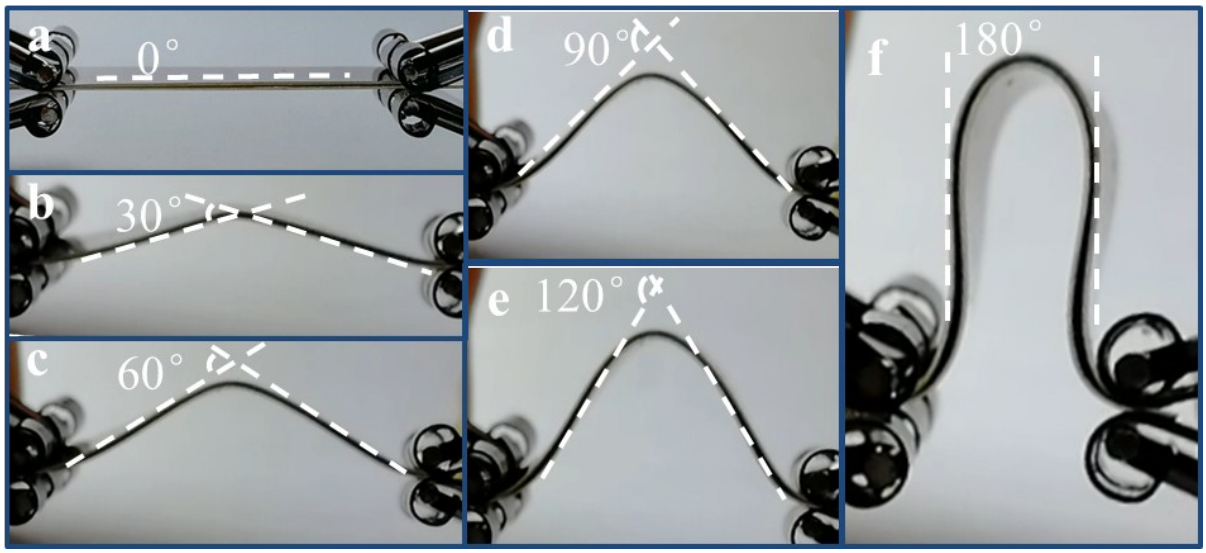

Figure S9 The photograph of flexible GeP_5 ASSP under different bending states (0 to 180°). 0° (a), 30° (b), 60° (c), 90° (d), 120° (e) and 180° (f).

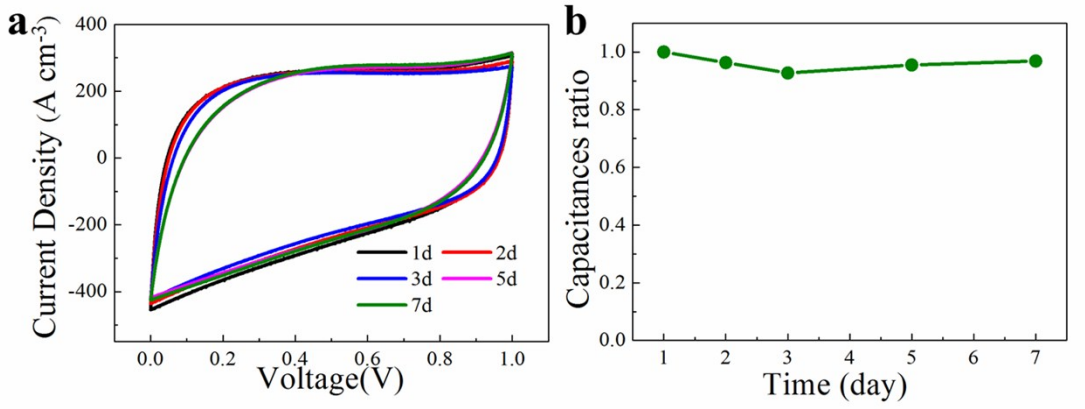

Figure S10 CV curves (a) and capacitances ratio (b) of GeP_5 ASSP exposed to air for a week.

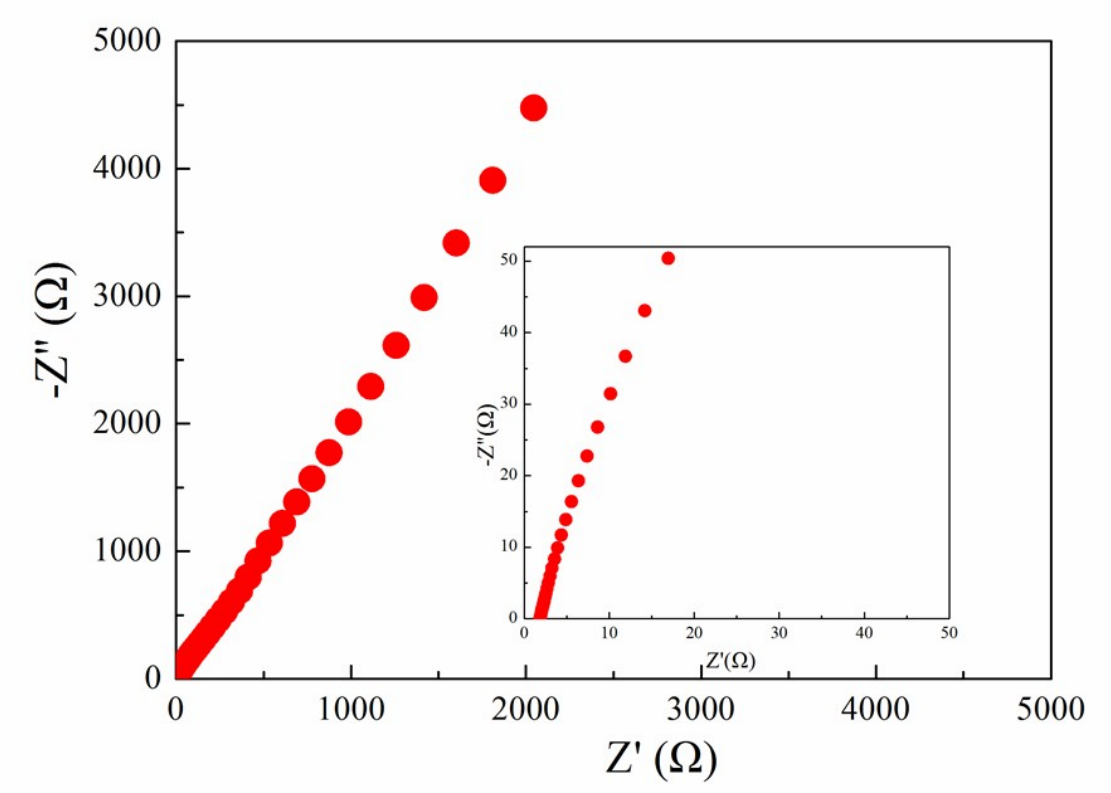

Figure S11 EIS of GeP_5 ASSP device. Inset shows the high frequency range part.

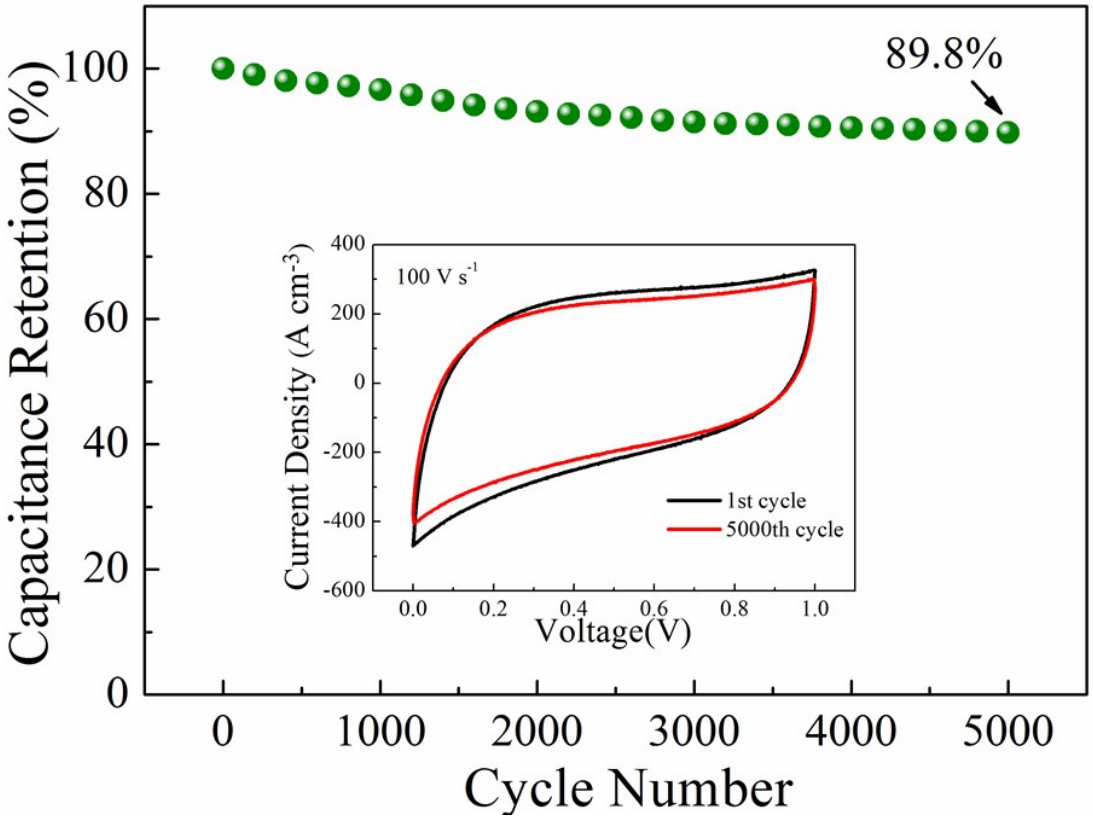

Figure S12 Capacitance retention of GeP_5 ASSP device at ultrahigh scan rate of 100 V s^{-1} after 5 000 cycles. Inset shows CV curves of the 1st cycle and 5 000th cycle.

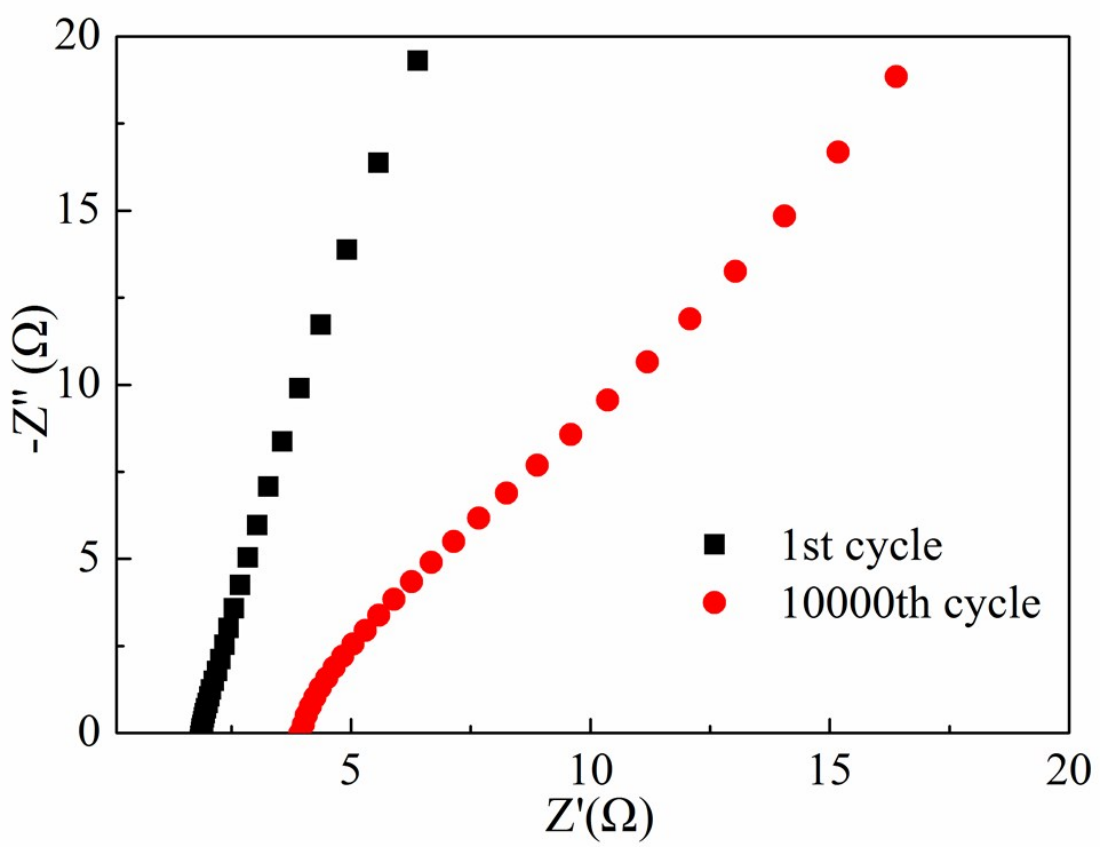

Figure S13 EIS tests of GeP_5 ASSP device after 1st cycle and 10 000th cycle.

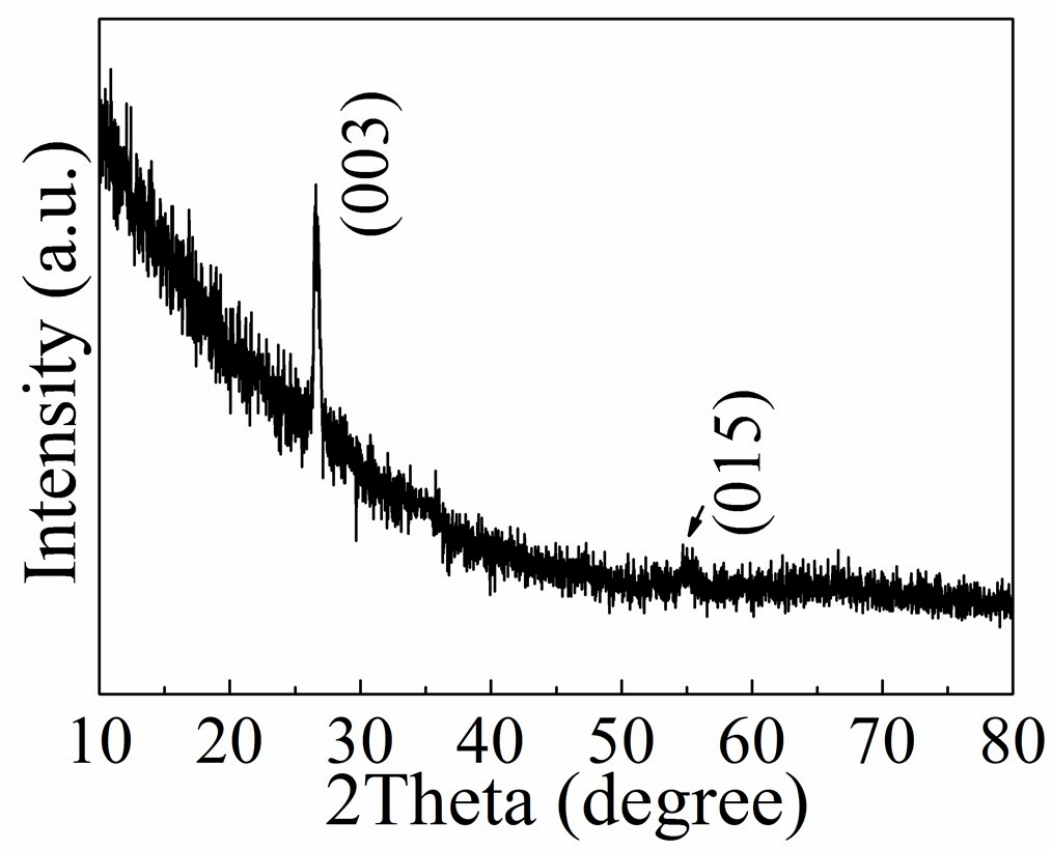

Figure S14 The XRD pattern of GeP_5 film after electrochemical measurements.

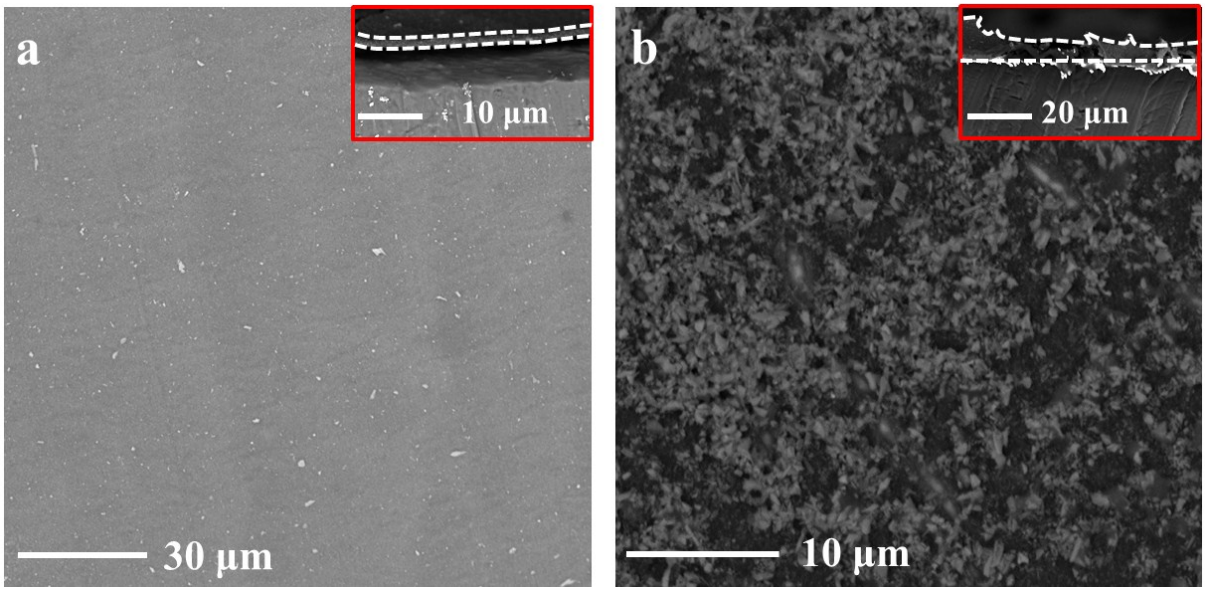

Figure S15 The SEM images of the GeP_5 electrode: (a) before cycling; (b) after cycling. The corresponding cross-section images are given as the insets.

Table S1 Comparison of 2D materials in terms of structure and electrical conductivity

Material	Structure	Electrical conductivity (S m^{-1})
Graphite[1]	$P6_3/mc$	3.3×10^2–2×10^5
BP[1]	$Cmca$	0.2–3.3×10^2
TiS_2[2]	$P\bar{3}m1$	1.4×10^5
WTe_2[3]	$Pmn2_1$	1.5×10^5
TaS_2[4]	$P6_3/mmc$	0.9-0.76×10^6
$TaSe_2$[4]	$P6_3/mmc$	0.833-0.71×10^6
NbS_2[4]	$P6_3/mmc$	0.83-1×10^6
$NbSe_2$[4]	$P6_3/mmc$	0.83-1×10^6
GeP_5	$R\bar{3}m$	2.4×10^6

Table S2 Comparison of the performance parameters (τ_0, f_o) of various ECs for AC-line filtering.

Electrode	τ_0 (ms)	f_o (Hz)	Electrolyte
GeP5 -SSCs	0.29	3390	Gel
ErGO - SSCs[5]	0.238	4210	Liquid
G/CNT - MSCs[6]	0.82	1343	Liquid
CNT - SSCs[7]	0.5	1995	Organic
EG/PH1000 - SSCs[8]	1.5	708	Gel
CB -SSCs[9]	1.56	641	Liquid
PiCBA - MSCs[10]	0.27	3620	Gel
PEDOT - MSCs[11]	3.3	400	Gel

SSCs sandwich-supercapacitors; MSCs: micro-supercapacitors; ErGO: electrochemical reduced graphene oxide; G/CNTCs: graphene/carbon nanotube carpets; CNTs: carbon nanotubes. EG/PH1000: grapheme/conducting polymer; CB: carbon black; PiCBA: azulenebridged coordination polymer framework; PEDOT: porous conducting poly (3, 4-ethylenedioxythiophene).

1 W. Li, H. Li, Z. Lu, L. Gan, L. Ke, T. Zhai and H. Zhou, *Energy Environ. Sci.* **2015**, 8, 3629.

2 L. E. Conroy and K. C. Park, *Inorg. Chem.* **1968**, 7, 459.

3 X. C. Pan, X. Chen, H. Liu, Y. Feng, Z. Wei, Y. Zhou, Z. Chi, L. Pi, F. Yen, F. Song, X. Wan, Z. Yang, B. Wang, G. Wang and Y. Zhang, *Nat. Commun.* **2015**, 6, 7805.

4 M. Naito and S. Tanaka, *J. Phys. Soc. Jpn.* **1982**, 51, 219.

5 K. Sheng, Y. Sun, C. Li, W. Yuan and G. Shi, *Sci. Rep*. **2012**, 2, 247.

6 J. Lin, C. Zhang, Z. Yan, Y. Zhu, Z. Peng, R.H. Hauge, D. Natelson and J.M. Tour, *Nano Lett.* **2013**, 13, 72.

7 Y. Yoo, S. Kim, B. Kim and W. Kim, *J. Mater Chem. A* **2015**, 3, 11801.

8 Z. S. Wu, Z. Liu, K. Parvez, X. Feng and K. Müllen, *Adv. Mater.* **2015**, 27, 3669.

9 P. Kossyrev, *J. Power Sources* **2012**, 201, 347.

10 C. Yang, K. S. Schellhammer, F. Ortmann, S. Sun, R. Dong, M. Karakus, Z. Mics, M. Löffler, F. Zhang, X. Zhuang, E. Cánovas, G. Cuniberti, M. Bonn and X. Feng, *Angew. Chem., Int. Ed*. **2017**, 129, 3978.

11 N. Kurra, M. K. Hota and H. N. Alshareef， *Nano Energy* **2015**, 13, 500.